ELSEVIER

Materials Chemistry and Physics 42 (1995) 143–147

MATERIALS CHEMISTRY AND PHYSICS

Materials Science Communication

Bandgap shrinkage of degenerate p-type GaAs by photoluminescence spectroscopy

M.S. Feng [a], C.S. Ares Fang [b], H.D. Chen [c]

[a] *Institute of Materials Science and Engineering, National Chiao-Tung University, Hsinchu, Taiwan, ROC*
[b] *SINONAR Co., 8 Prosperity Road 1, Science-Based Industrial Park, Hsinchu, Taiwan, ROC*
[c] *Institute of Electronics, National Chiao-Tung University, Hsinchu, Taiwan, ROC*

Received 23 December 1994; revised 13 April 1995; accepted 21 April 1995

Abstract

Photoluminescence characteristics of heavily carbon-, beryllium- and zinc-doped GaAs were studied in this investigation. The band-to-acceptor (e,A) transition was identified via various doping concentrations from 10^{17} to 10^{20} cm^{-3} and the temperature from 20 to 300 K. As a result the (e,A) peak was found to be a dominant peak at 20 K instead of the band-to-band (B,B) peak at $p > 1 \times 10^{19}$ cm^{-3}. The (e,A) peak was also observed at 300 K and enhanced with the increasing carrier concentration at $p > 2.8 \times 10^{18}$ cm^{-3}. Bandgap shrinkage of these samples was qualitatively obtained. When $p > 1 \times 10^{19}$ cm^{-3}, the impurity band merges with the valence band and the binding energy of the acceptor is equal to zero. Consequently, the bandgap can be taken as the energy between the conduction-band minimum and the top of the impurity band.

Keywords: Photoluminescence; Spectroscopy; Bandgap shrinkage; GaAs

1. Introduction

Heavily doped materials are of interest for pursuing either low base resistance of highly conductive contacts for the heterojunction bipolar transistors (HBTs) [1–6]. In heavily doped GaAs, due to the Coulomb interaction between the ionized impurities and holes, and the exchange energy of the hole shift, the band edge changes from its undoped value E_0 into the bandgap by ΔE_v [7]. Several methods to determine the bandgap shift caused by heavy doping are available. However, each method is subject to limitation. Determination of the bandgap shift from a transport device structure is difficult due to the many parameters such as mobility, lifetime and diffusion constant which are not easy to measured [7,8]. Standard absorption measurement cannot be used to measure the band-to-band (B,B) absorption for the heavily doped epilayers due to the Burnstein–Moss effect [9]. Other methods, such as the capacitance method [10] and X-ray photoemission spectroscopy [11], were also used to deduce the shift in bandgap structure.

Photoluminescence (PL) is a common technology to investigate the bandgap properties of the III–V semiconductors [2,3,9,12,13]. Olego and Cardona [12] studied the PL characteristics of the heavily Zn-doped GaAs single crystal and proposed a method to decide the real bandgap of the heavily doped material. The energy corresponding to the tail of the main emission band and the background is taken as the 'actual bandgap' of the material. The method has been used to decide the bandgap of heavily C-doped [2,3,9] and Be-doped [13] GaAs samples. It is valid if the main peak is due to the (B,B) transition. When the doping concentration is at the light and medium doping levels, the (B,B) and band-to-acceptor (e,A) transitions are both possible [14,15]. However, for the heavily doped regime, the impurity band merges with the valence band; in this situation, the existence of the (e,A) peak is arguable [14–16]. Additionally, the PL lineshapes of the samples grown by metal-organic chemical vapor deposition (MOCVD) [2,3,5,9] are also different from the samples of the Zn-doped single crystals GaAs [12] at the heavily doped regime.

In this investigation, we varied the measured temperature and concentration to identify the (e,A) peak. The bandgap shrinkage of degenerate p-type GaAs is discussed.

2. Experimental

Both the C- and Zn-doped layers were grown in a low-pressure (50 Torr) triethylgallium–arsine ($TEGa$-AsH_3) base MOCVD system. A horizontal thermoresistor heater was

SSDI 0254-0584(95)01566-D

used for growth process. The source materials were TEGa, AsH_3, diethylzinc (zinc doping source) and CCl_4 (carbon doping source). The details of LP-MOCVD growth characteristics have been described in a previous study [6]. The Be-doped GaAs was grown by solid-source molecular beam epitaxy (MBE). All samples were grown on Cr-doped semi-insulation GaAs (100) substrates. The carrier (hole) concentrations were measured by the standard van der Pauw–Hall method at a magnetic field of 5 kG. Optical transitions were studied by PL measurement. The PL spectra were obtained with the 4880 Å line of an Ar^+ laser at an excitation intensity of 160 mW from 300 to 20 K.

3. Results and discussion

Fig. 1 shows the PL spectra of undoped GaAs at 20 K with different acceptor concentrations as a reference for the PL measurements. Since the relationship between the acceptor (carbon) concentrations of the four samples is $[C]_{(a)} > [C]_{(b)} > [C]_{(c)} > [C]_{(d)}$, the peak at 1.489 eV can be identified as the (e,A) peak, and the peak at 1.514 eV identified as the (B,B) peak [6]. Fig. 2 illustrates the normalized PL spectra at 20 K of the sample with $p = 1.3 \times 10^{17}$ to 1.4×10^{20} cm^{-3}. The two samples with $p = 1.3 \times 10^{17}$ and 5×10^{17} cm^{-3} are the Be-doped GaAs films, and the other samples are the C-doped GaAs. For further concentration increases up to 5×10^{17} cm^{-3}, the (B,B) peak is at higher energy beside the (e,A) peak, but it is not very noticeable. For the concentrations between 1.3×10^{17} and 5×10^{17} cm^{-3}, the (e,A) peak is observed higher than that of the (B,B) peak

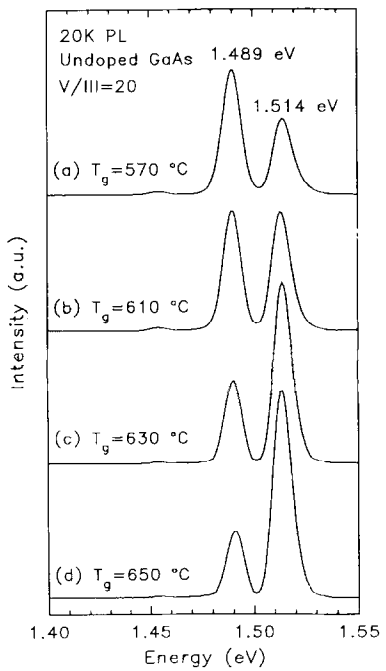

Fig. 1. PL spectra of the undoped GaAs at 20 K with different acceptor concentrations. The relationship between the acceptor (carbon) concentrations of the four samples is $[C]_{(a)} > [C]_{(b)} > [C]_{(c)} > [C]_{(d)}$.

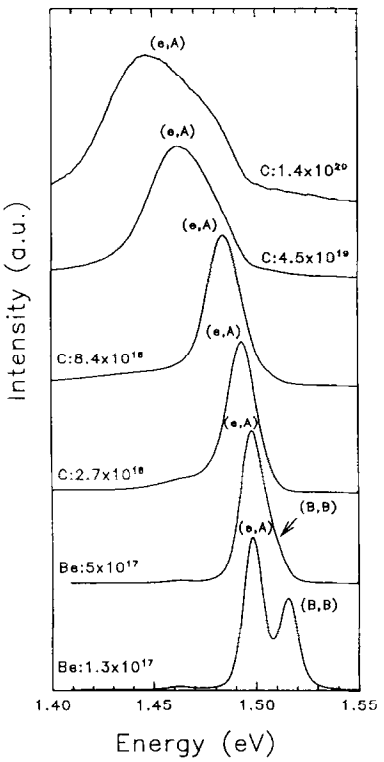

Fig. 2. Normalized PL spectra of the C- and Be-doped GaAs with $p = 1 \times 10^{17}$–1.4×10^{20} cm^{-3} at 20 K. The (e,A) peak grows, relative to the (B,B) peak, with the increasing hole concentration.

at 30 K for the sample of $p = 2.7 \times 10^{17}$ cm^{-3} [13]. More rapid increase in the (e,A) peak than the (B,B) peak, as with the increasing acceptor concentration, leads to the disappearance of the (B,B) peak at $p > 5 \times 10^{17}$ cm^{-3}. In Fig. 2, the main peak is due to the (e,A) peak and its shift toward low energy. It becomes broader as the hole concentration increases.

Fig. 3 shows the Be-doped GaAs sample with $p = 1.3 \times 10^{17}$ cm^{-3} at 100 and 20 K, respectively. The overall intensity decreases as the temperature increases. The intensity decreasing rate of the (e,A) peak is higher than that of the (B,B) peak, leading to the fact that the (e,A) peak is lower than the (B,B) peak at 100 K. In addition, the width of the (B,B) peak becomes broader and merges with the (e,A) peak.

The temperature dependence of PL spectra at $p = 8.4 \times 10^{18}$ cm^{-3} is illustrated in Fig. 4. The intensity of the low-energy peak increases faster than that of the high-energy peak with decreasing temperature. This would lead towards the domination of a lower-energy peak at a lower temperature. The higher-energy peak is due to the (B,B) transition that has been described in many studies [12,13,17,20,25]. The low-energy peak has been controversial in many studies [17,26,27]; this is the (e,A) transition shown in Fig. 4. The temperature dependences of the (e,A) peak and (B,B) peak of C-doped GaAs are the same as those of Be-doped GaAs.

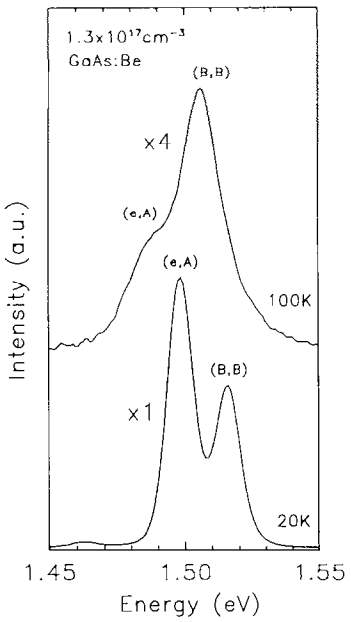

Fig. 3. Be-doped GaAs with $p = 1.3 \times 10^{17}$ cm^{-3}. The (e,A) peak and the (B,B) peak still separate at 20 K; however, these two peaks merge due to the broadening of the (B,B) peak as the temperature reaches 100 K.

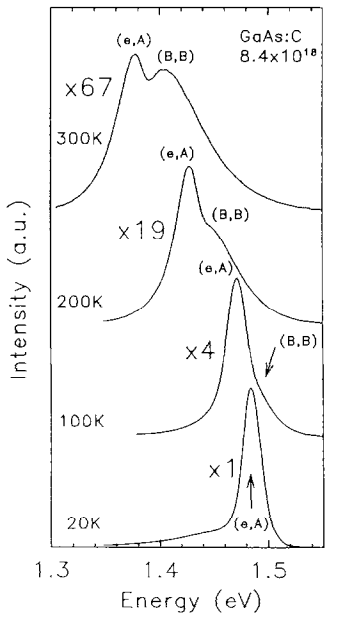

Fig. 4. PL spectra of the C-doped GaAs with $p = 8.4 \times 10^{18}$ cm^{-3}. The (B,B) peak is observed at $T \geqslant 100$ K.

As mentioned above, the (e,A) peak is enhanced with increasing acceptor concentration and it dominates the 20 K emission spectrum when $p \geqslant 5 \times 10^{17}$ cm^{-3}. Additionally, when $p \geqslant 8.4 \times 10^{18}$ cm^{-3}, the (e,A) peak is higher than the (B,B) peak at 300 K, and it dominates the 300 K spectra. Fig. 5 illustrates the 300 K PL spectra of the C-doped samples with $p = 2.7 \times 10^{18}$, 8.4×10^{18} and 8.9×10^{19} cm^{-3}, respectively. The intensity of the (e,A) peak relative to the (B,B) peak increases with hole concentration and leads to the appearance of the (e,A) peak at 300 K which dominates the luminescence spectrum. When $p = 2.7 \times 10^{18}$ cm^{-3}, the low-energy peak is only a shoulder peak beside the (B,B) peak, where both the (e,A) peak and the (B,B) peak can be observed at $p = 8.9 \times 10^{19}$ cm^{-3}. In other words, the (e,A) and (B,B) peaks occur at the heavily doped level, in which the impurity band merges with the valence band (e.g., $p \geqslant 1.5 \times 10^{19}$ cm^{-3} [22]). In previous studies, it is arguable that the (e,A) peak does not appear in the PL spectrum of heavily doped GaAs. Of course, the lower-energy peak of the spectra from other MOCVD-grown samples [2,3,5,9] must be due to the (e,A) peak.

The appearance of the (e,A) peak at 300 K dominating the low-temperature emission spectrum can be explained as follows. Since the carbon acceptors can all be ionized at a light doping level, the recombination of photo-created electrons through the available acceptor holes can be negligible at this doping level. Therefore, recombination though acceptors (band-to-acceptor transition) cannot be observed. When the number of dopant ions is higher than the number of thermal-equilibrium electrons, the acceptors cannot be fully ionized. The electrons can be recombined through the unionized acceptor holes. Hence, the (e,A) peak is observed at room temperature in the heavily doped samples. Fig. 5 illustrates this point as the (e,A) peak is clearly seen at $p \geqq 8.4 \times 10^{18}$ cm^{-3}. In addition, the number of thermally created electrons decreases as the temperature is decreased, resulting in the increase of unionized acceptors. The probability of transition through acceptors is then increased. It is found that the luminescence intensity of the (e,A) peak relative to the (B,B) peak is enhanced with reduced temperature.

Fig. 6 illustrates the PL spectra of the Be-doped GaAs spectra at four different temperatures. The spectrum is composed of the (e,A) peak and the (B,B) peak, but these two peaks are too close to be differentiated clearly. The Zn-doped GaAs has the same trend as the C-doped GaAs, except that the peak position was slightly lower than that of the C-doped GaAs [23]. The PL spectra from the Zn-doped GaAs substrate also show one luminescence peak from low temperature to high temperature, which is consistent with the results from

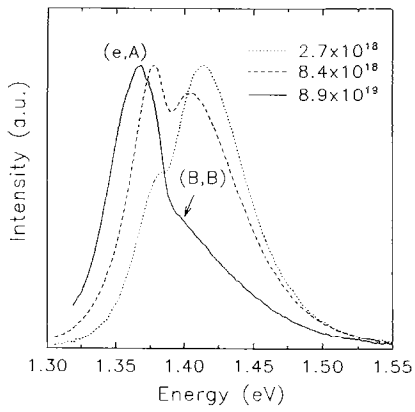

Fig. 5. PL spectra at 300 K of the C-doped GaAs with $p = 2.7 \times 10^{18}$, 8.4×10^{18} and 8.9×10^{19} cm^{-3}, respectively. The intensity of PL spectra is normalized.

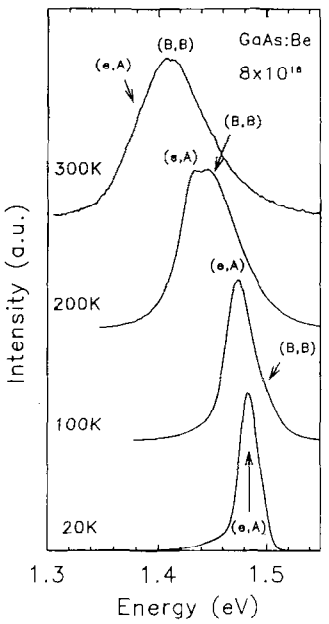

Fig. 6. Be-doped GaAs with $p = 6 \times 10^{18}$ cm^{-3}. The (e,A) peak is found at 20 K, and the (B,B) peak is observed at $T \geqslant 200$ K. The (e,A) peak at the low-energy side of the (B,B) peak is not apparent.

Olego and Cardona [12]. The (e,A) transition must occur for the Zn-doped substrate. However, since these two luminescence bands are so close, the luminescence band exhibits only one peak, which is similar to the Be-doped sample shown in Fig. 6, otherwise the width of the (e,A) peak from the substrate is broader than that from the epitaxial layers, such as C-doped GaAs.

The linewidth of the (B,B) peak is broader than that of the (e,A) peak. Both peaks become broader as the doping concentration is increased. However, the increasing rate of the (B,B) peak linewidth is greater than that of the (e,A) peak when the temperature increases. The 300 K spectrum of the (B,B) peak has an asymmetric structure with low-energy cut-off. As the doping concentration increases, the low-energy cut-off properties are destroyed, and a band tail extends toward both lower-energy and high-energy sides. The extension of the high-energy band tail toward the high-energy side is higher than the intrinsic bandgap due to the hot electron luminescence [5]. When the band tail is extended to low energy and is overlapped with the (e,A) peak, the position and the height of the (e,A) peak and the (B,B) peak are not precise. Because of these phenomena, it is difficult to identify the precise positions of both the (e,A) peak and the (B,B) peak.

Both the (e,A) and (B,B) peaks shifts to low energy as the dopant concentration are increased. The peak shift toward low energy is due to the bandgap narrowing [7,12]. Fig. 7 demonstrates the 'bandgap narrowing' of the heavily C-doped GaAs at three different temperatures. Data reported by other groups [12,13] are also shown in the figure for comparison. Bandgap narrowing is the deviation between the intrinsic bandgap and the 'actual bandgap'. The intrinsic

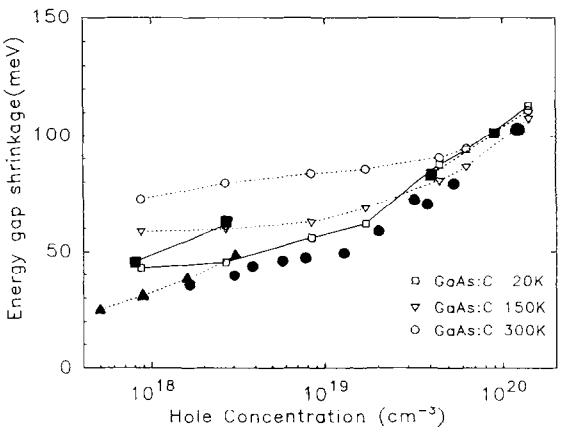

Fig. 7. Band gap shrinkage of the C-doped GaAs. ■, Olego [12]; ▲, Borghs [13]; ●, Hanna [2].

bandgap was calculated from the Varshni equation [12]:

$$E(T) = 1.519 - \frac{5.04 \times 10^{-4} T^2}{204 + T} \quad (1)$$

The intersection between the tangent to the low-energy tail of the main emission peak and the background of the PL spectrum is equal to the 'actual bandgap' of the heavily doped materials [9]. This rule is based on the main emission peak due to the (B,B) transition. The method has been widely used to decide the bandgap of the heavily C-doped GaAs [2,3]. However, for heavily C-doped GaAs, as mentioned above, the main emission peak is due to the (e,A) peak. Then, the method must be modified to suit the C-doped GaAs.

The energy gap shown in Fig. 7 for C-doped GaAs is the energy gap between the conduction band minimum and the top of the impurity hand. Then, the 'bandgap narrowing' is independent of temperature when $p > 10^{19}$ cm^{-3}. The electrical characteristics show that the impurity band merges with the valence band at about 10^{19} cm^{-3} [21] from the varying temperature resistivities. For heavily doped concentrations ($p > 1 \times 10^{19}$ cm^{-3}), the linewidth of the (B,B) peak becomes broader. Its band tail moves toward the forbidden band and reaches the top of the (e,A) luminescence band edge. In this concentration range, the impurity band tail and the valence band tail overlap, but it does not imply that these two bands are overlapped. The densities of the hole states [23] are not in the same distribution energy for these two bands. However, the bandgap energy is the energy between the conduction band minimum and the top of the impurity band. For $p < 10^{19}$ cm^{-3}, the relative peak intensity between the (e,A) peak and the (B,B) peak depends on temperature. Bandgap shrinkages of these samples cannot be quantitatively obtained by using the rule which takes the intersection between the tangent to the low-energy tail of the main emission peak and the background of the PL spectrum as the 'real bandgap' of heavily doped materials.

4. Conclusions

The (B,B) transition and the (e,A) transition have been identified and investigated. The low-temperature domination peak is the (e,A) transition instead of the previous identification of the (B,B) peak. This can be observed in the degenerate p-GaAs at 300 and 20 K. Not only does the band tail of the (B,B) peak shift toward low energy, but also the (e,A) peak. For $p < 10^{19}$ cm^{-3}, the bandgap narrowing can be qualitatively obtained. The impurity band merges with the valence band at about $p = 10^{19}$ cm^{-3}. Thus, the bandgap is the energy between the conduction minimum and the top of the valence band.

Acknowledgements

This work was supported by the National Science Council of Taiwan, Republic of China, under contracts NSC-82-0417-E-009-348 and NSC-83-0417-E-009-016.

References

[1] G.W. Wang, R.L. Pierson, P.M. Asbeck, K.C. Wang, N.L. Wang, R. Nubling, M.F. Chang, J. Salerno and S. Sastry, *IEEE Trans. Electron Device Lett., 12* (191) 347.
[2] M.C. Hanna, Z.H. Lu and A. Majerfeld, *Appl. Phys. Lett., 58* (1991) 164.
[3] L.W. Yang, P.D. Wright, V. Eu, Z.H. Lu and A. Majerfeld, *J. Appl. Phys., 72* (1993) 2063.
[4] B.J. Cunningham, M.A. Haase, M.J. Mccollum, J.E. Baker and G.E. Stillman, *Appl. Phys. Lett., 54* (1989) 1905.
[5] B.J. Aithison, N.M. Haegel, C.R. Abernathy and S.I. Pearton, *Appl. Phys. Lett., 56* (1990) 1154.
[6] H.D. Chen, C.Y. Chang, K.C. Lin, S.H. Chan, M.S. Feng, P.A. Chen, C.C. Wu and F.Y. Juang, *J. Appl. Phys., 73* (1993) 7851.
[7] M.S. Lundström, M.E. Klausmeier-Brown, M.R. Melloch, R.K. Ahrenkiel and B.M. Keyes, *Solid State Electron., 33* (1990) 693.
[8] M.E. Klausmeier-Brown, M.R. Melloch and M.S. Lundström, *J. Electron. Mater., 19* (1990) 7.
[9] L. Wang, B.J. Aitchison and N.M. Haegel, *Appl. Phys. Lett., 60* (1992) 1111.
[10] P. Van Mieghem, R.P. Mertens, G. Borghs and R.J. Van Verstraeten, *Phys. Rev. B, 41* (1990) 52 952.
[11] J.A. Silberman, T.J. de Lyon and J.M. Woodall, *Appl. Phys. Lett., 58* (1991) 2126.
[12] D. Olego and M. Cardona, *Phys. Rev. B, 22* (1980) 22.
[13] G. Borghs, K. Ghattacharyya, K. Deneffe, P. Van Mieghem and R. Mertens, *J. Appl. Phys., 66* (1989) 4381.
[14] D.A. Cusano, *Solid State Commun., 2* (1964) 353.
[15] D.N. Nasledov, A.A. Rogachev, S.M. Ryvkin, V.E. Khartsiev and B.V. Tsarenkov, *Sov. Phys. Solid State, 4* (1962) 2449.
[16] R.C. Miller, D.A. Kleinman, W.A. Nordland, Jr. and R.A. Logan, *Phys. Rev. B, 23* (1981) 4399.
[17] D.M. Szmyd and A. Majerfeld, *J. Appl. Phys., 65* (1989) 1788.
[18] P.W. Yu and E. Kuphal, *Solid State Commun., 49* (1984) 907.
[19] A. Louati, C. Charreaux, A. Nouailhat, G. Guillot, P.N. Farennec and M. Salvi, *Solid State Commun., 62* (1987) 31.
[20] F.E. Rosztoczy, F.E. Ermanis, I. Hayashi and B. Schowartz, *J. Appl. Phys., 41* (1970) 264.
[21] H.D. Chen, M.S. Feng, P.A. Chen, C.C. Wu and J.W. Wu, *Jpn. J. Appl. Phys., 33* (1994) 1920.
[22] A.N. Titkov, E.I. Chalkina, E.M. Komova and N.G. Ermakova, *Sov. Phys. Semicond., 15* (1981) 198.
[23] H.D. Chen, M.S. Feng, P.A. Chen, K.C. Lin and C.C. Wu, *J. Appl. Phys., 75* (1994) 2210.
[24] H.D. Chen, M.S. Feng, K.C. Lin, P.A. Chen, C.C. Wu and J.W. Wu, *J. Appl. Phys.*, (1994).
[25] M. Bugajski and W. Lewandowsik, *J. Appl. Phys., 57* (1985) 521.
[26] U. Langman and U. Kenig, *J. Phys. Chem. Solids, 36* (1975) 1067.
[27] W.N. Carr and J.R. Biard, *J. Appl. Phys., 35* (1964) 2776.